This is an *Accepted Manuscript*, which has been through the Royal Society of Chemistry peer review process and has been accepted for publication.

Accepted Manuscripts are published online shortly after acceptance, before technical editing, formatting and proof reading. Using this free service, authors can make their results available to the community, in citable form, before we publish the edited article. We will replace this *Accepted Manuscript* with the edited and formatted *Advance Article* as soon as it is available.

You can find more information about *Accepted Manuscripts* in the **Information for Authors**.

Defect Stabilized Gold Atoms on Graphene as Potential Catalysts for Ethylene Epoxidation: A First-principles Investigation

Xin Liu†, Yang Yang†, Minmin Chu†, Ting Duan†, Changgong Meng† and Yu Han‡,**

† School of Chemistry, State Key Laboratory of Fine Chemicals, Dalian University of Technology, Dalian, 116024, P. R. China.

‡ Physical Sciences and Engineering Division, Advanced Membranes and Porous Materials Center, King Abdullah University of Science and Technology, Thuwal, 23955-6900, Saudi Arabia

---

*Corresponding Authors:

Dr. Xin Liu and Prof. Yu Han

Tel: +86-411-84986343(X. L.); +966-2-8082407 (Y. H.)

Email: xliu@dlut.edu.cn (X. L.); yu.han@kaust.edu.sa (Y. H.)

ABSTRACT

   We performed a first-principles based investigation on the potential role of Au atoms stabilized by defects on graphene in ethylene epoxidation. We showed that the interactions between the Au atoms and vacancies on graphene not only turn the Au atomic diffusion a 2.10 eV endothermic process, but also tune the energy level of Au-d states for the activation of O_2 and ethylene and promote the formation and dissociation of the peroxametallacycle intermediate. The catalytic cycle of ethylene epoxidation is initiated with the formation of a peroxametallacycle intermediate by the coadsorbed ethylene and O_2, through the dissociation of which an ethylene epoxide molecule and an adsorbed O atom are formed. Then, gaseous ethylene reacts with the remnant O atom directly for formation of another ethylene epoxide molecule. The desorption of ethylene epoxide is facilitated by subsequent adsorption of O_2 or ethylene and a new reaction cycle initiates. The calculated energy barriers for the formation and dissociation of peroxametallacycle intermediate and regeneration of Au sites are 0.30, 0.84 and 0.18 eV, respectively and are significantly lower than those for aldehyde formation. These findings suggest the potential high catalytic performance of these Au atoms for ethylene epoxidation.

KEYWORDS: Graphene; monovacancy; defects; Au; ethylene; oxidation;

Catalysis Science & Technology Accepted Manuscript

1. INTRODUCTION

Ethylene oxide (EO) is an important commodity chemical.[1] It is used not only for production of ethylene glycol and surface-active agents such as nonionic alkylphenol ethoxylates and detergent alcohol ethoxylates, but also as the raw materials for several dozen important fine petroleum and chemical intermediates. Currently, EO is produced through vapor phase ethylene epoxidation over Ag supported on α-Al_2O_3 with alkali metal additives and Cl as promoters and the EO selectivity can reach 90%, while the EO selectively over pure Ag is only 40–50%.[2-3] The global market for EO is expected to exceed 27 million tons by the year 2017.[4] Due to the huge global capacity of this process, even slight improvements in the selectivity would result in significant economical benefits.

In epoxidation of ethylene, the selectivity to EO is controlled by a reaction network of competing elementary pathways where a surface oxametallacycle ($-OCH_2CH_2-$, OMC) intermediate undergoes isomerization reactions. The selective OMC ring closure produces the EO, whereas nonselective hydride transfer within the $-CH_2CH_2-$ leads to formation of acetaldehyde which undergoes facile nonselective combustion to CO_2 and H_2O due to the high reactivity of the aldehydic C-H bond as well as the three equivalent α-H next to the aldehyde group.[2-3, 5-8] The selectivity to EO is found sensitive to the exposed transition metal (TM) facets,[8-9] the size of the TM nanoparticles (NPs),[10] the detailed coordination at the reaction sites, the composition of the reaction mixture[11] and etc.[6] Many approaches have been developed to achieve higher selectivity to EO, including morphology and size control of the TM NPs, alloying with different TMs and the utilization of novel promoters.[10-17] Au is also a Group IB metal but has long been considered to be catalytic inert due to its nobleness in bulk form. Torres et al studied the epoxidation mechanism of ethylene on an oxygen-atom-covered Au(111) surface

theoretically.[18] They showed that the predicted selectivity of ethylene epoxidation on Au(111) is ~40% and is similar to that on Ag(111).[2] Au NPs have attracted considerable interest due to their distinctly different catalytic properties as compared with the bulk.[19-20] Au NPs supported on reducible metal-oxides showed high activity for oxidation of CO[21] and alkene[22-23] at low temperature and the activity can be modulated with reductive component in the mixture and even water.[11, 24] Freestanding Au NPs and Au NPs supported on inert materials are also efficient and robust for selective oxidation of styrene. [11, 20, 25-27] These make supported Au NPs alternative catalysts for ethylene epoxidation.

For deposited TM NPs for heterogeneous catalysis, downsizing the TM NPs size and keeping them finely dispersed is highly desired to maintain a higher density of reaction sites for better conversion and so as the catalytic performance.[28] Due to the localized nature of TM-d states, their sensitivity to the local coordination and domination on the reactivity of TM NPs, the exposed unsaturated TM atoms are the reaction centers and the catalytic performance depends more strongly on the morphology than the size of TM NPs.[29-31] As the size of NPs goes down, the TM-support interaction may not only alter the spacial and energetic distribution of TM states that are essential for adsorption and activation of the adsorbates, [32-33] but also strongly impact the free energy of the assembly of TM atoms that sets the atomic stacking, the morphology and the durability of the TM NPs.[27, 34-36] Following this, several single-atom catalysts, such as Au/FeO_x,[37-38] Au/ZrO_2,[39] Pd/CeO_2,[40] $Ir/Fe(OH)_x$,[41] Ag/MnO_x,[42] $Fe/SiCO_x$[43] and etc, have been fabricated and proved efficient in reactions, including CO oxidation, hydrogenation of butadiene, methanol reforming, NO reduction, conversion of methane and etc. A thorough understanding of the TM-support interactions would be vital for the design of supported sub-nano TM NPs or even single TM atoms as catalysts for a specific reaction.

Many studies showed that defects of the supports could serve as anchoring sites for TM atoms. The defects, including dopants, vacancies and etc in graphene have been proposed to modulate the electronic structures and so as the catalytic performance of supported TM NPs and atoms.[32, 44-46] Recently, heteroatom-embedded graphene was fabricated,[47] while Au, Cu, Fe and Pt atoms embedded in graphene have been proposed to be efficient for CO and olefin oxidation.[11, 48-51] These investigations provide strong evidence that fabrication of mono-dispersed single TM atom catalyst by defect engineering of the support materials is feasible and the resulting catalyst may display unusual behaviors compared with conventional catalysts.

Inspired by these works, we performed a first-principles-based investigation on potential role of Au atoms dispersed on graphene in ethylene epoxidation. We showed the defects on graphene interact with Au atoms strongly and turn the atomic diffusion processes highly endothermic. This strong interfacial interaction also tunes the Au-d states for the adsorption and activation of O_2 and ethylene. The epoxidation of ethylene involves the formation and dissociation of a peroxametallacycle intermediate ($-O-O-CH_2-CH_2-$) through which an ethylene epoxide molecule and an adsorbed O atom are formed. Subsequent reactions take place between gaseous ethylene and the remnant O atom and re-initiate the catalytic cycle. The calculated energy barriers for the formation and dissociation of the peroxametallacycle intermediate and regeneration of Au site are 0.30, 0.84 and 0.18 eV, respectively and are significantly lower than those for aldehyde formation, suggesting the potential high catalytic performance of these mono-dispersed Au atoms for ethylene epoxidation. The rest of the paper is organized as the following: the theoretical methods and computational details are described in Section 2, the results are presented and discussed in Section 3 and concluded in Section 4.

2. THEORETICAL METHODS

First-principles based calculations were performed using GGA-PBE functional with DSPP pseudopotentials as implemented in DMol^3.[52-55] A hexagonal 6 × 6 supercell of pristine graphene was used to mimic the graphene and the Au-graphene composites. The minimum distance between the graphene sheet and its mirror images is set to be larger than 20 Å to avoid the interactions among them. We used empirical potential for pre-optimization,[56-57] and these preoptimzed structures were fully relaxed in DMol^3 until the forces were below 1×10^{-2} eV/Å. The transition states were located through the synchronous method with conjugated gradient refinements.[58] For all calculations, the real-space global orbital cutoff radius was set to 4.6 Å and the energy convergence criterion was 2×10^{-4} eV. A Γ centered 2 × 2 × 1 k-point grid was used for geometry optimization and transition state search, while a 20 × 20 × 1 k-point grid was used for electronic structure analysis.[59] The Hirshfeld scheme was adapted to estimate the charge transfer.[60] With the above setup, the minimum C-C distance in pristine graphene is 1.42 Å.[61]

The binding energy (E_b) of an Au atom onto graphene(GN) is calculated as the energy difference between the Au-graphene composite (AuGN) and the clean GN substrate plus the freestanding Au atom, following Equation (1).

$$E_b = E_{AuGN} - (E_{Au} + E_{GN}) \qquad (1)$$

For the study concerning adsorption of ethylene, O_2, O, ethylene epoxide, acetaldehyde and etc., the adsorption energy (E_{ad}) is calculated as the energy difference between the species absorbed AuGN and the gaseous species plus the bare AuGN, following Equation (2).

$$E_{ad} = E_{adsorbate+AuGN} - (E_{AuGN} + E_{adsorbate}) \ (2)$$

3. RESULTS AND DISCUSSIONS

We started with the investigation on the dispersion of Au atoms onto pristine graphene (PGN) and found Au atoms bind weakly with PGN. The deposition of an Au atom on top of a C atom is at most 0.03 eV more plausible as compared with the other sites considered. In this configuration, Au atom stands 2.55 Å above a C atom and a corrugation of 0.15 Å in PGN is formed due to the Au-C interaction. The calculated E_b is -0.10 eV and the charge transfer to PGN is 0.11 $|e|$. The small differences among the E_bs at various deposition sites(0.03 eV), the low atomic diffusion barrier (0.03 eV) and the small charge transfer (0.11 $|e|$) suggest the easiness for atomic diffusion and aggregation for formation of large NPs on PGN as a result of the large surface energy of these mono-dispersed Au atoms.[36, 62] One possible solution to this is to stabilize the Au atoms by forming mature interactions with the graphenic substrate to turn the atomic diffusion into a demanding process in conventional environment. The wide variety of atomic defects on chemically synthesized graphene samples, including clustered pentagons and heptagons, vacancies, edges and contaminations, provide an immediate solution in this category.[63] We recently found that these localized defect structures on reduced graphene oxide can act as strong trapping sites for TM NPs and inhibit their aggregation.[27, 33] As the other defects can be considered as derivatives of single vacancy (SV) and its stability is similar to that of divacancy, it is typical for analyze the defective graphene-TM interaction.

Due to the larger size of Au atoms as compared with C atoms, when an Au atom is placed above a SV, it is 2.16 Å above the basal plane of graphene after geometry optimization. The charge on Au atom at the SV (AuSV) is enhanced to 0.35 $|e|$ as compared with that on PGN (0.10 $|e|$). The differential charge density showed that there are significant charge accumulation regions between the Au atoms and the neighboring C atoms, suggesting the formed interactions are

partially covalent (Figure 1a). The DOS of SV is characterized with sharp peaks around E_F associated with the dangling bonds at SV.[32, 64] After Au deposition, the peaks at the E_F are shifted downwards, got occupied and broadened, and overlap with the peaks of Au-sp and Au-d states, showing the strong hybridization among them. (Figure 1c) This, together with the differential charge density, suggests that the Au atom uses its valence states to interact with the dangling bonds of the SV. The E_b at SV (-2.20 eV) is thus enhanced by more than twenty folds as compared with that on PBN (-0.10 eV). The enhanced E_b also makes the outward diffusion of Au atom to the top of its neighboring C atoms endothermic by 2.10 eV and is much higher than the Au atomic diffusion barrier of 0.03 eV on PGN, so the diffusion of SV stabilized Au atoms is kinetically prohibited in conventional environment. This binding, though is 1.73 eV less significant as compared with the calculated bulk cohesive energy of Au (3.83 eV),[65] still kinetically facilitates AuSV as the initial anchor points for the growth of Au NPs as proved by the recent findings that Au NPs can be stabilized on defective graphene whose growth may be manipulated with concentration of Au precursors used.[27, 66]

The spin density of AuSV (Figure 1b) is localized on the Au atom and is mainly contributed by the in-plane components of Au-d states and the C-sp states of C atoms around SV. This, in accordance with the DOS analysis, confirms that some of the partially occupied dangling Au-d states are localized at E_F and resonance with C-sp states due to the Au-C interaction. The energy levels of localized d states of transition metals are known vital for the activation of adsorbed reactants and subsequent reactions.[29] The dominant contribution of Au-d states at E_F suggest that the transfer of electrons from AuSV for activation of adsorbates would be much easier as compared with bulk Au. In this sense, AuSV may exhibit higher reactivity in activation of adsorbed ethylene and O_2 for ethylene epoxidation.
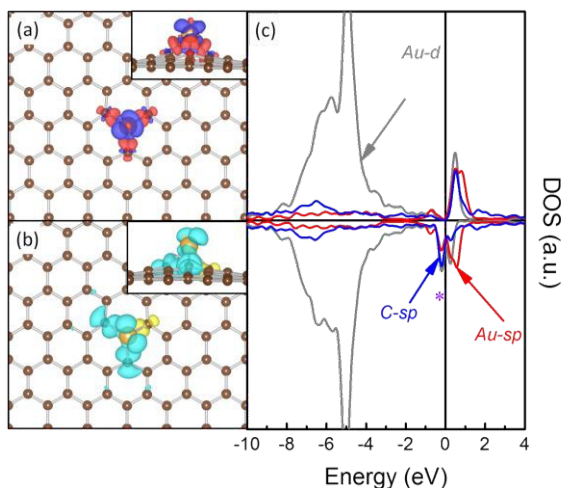
Figure 1. Structure and contour plots of differential charge density (a), spin density (b) and DOS of AuSV (c). (C: Brown; Au: Dark yellow. The contour values in (a) and (b) are ± 0.005 a.u. The charge accumulation regions are in red while the charge depletion regions are in blue. The major spin density is in light yellow while the minor spin density is in light blue.)

We then investigated the adsorption of reaction species to deduce the thermodynamics of the reaction (Table 1 and Figure 2). For ethylene epoxidation over AuSV, the key reaction species are O_2, ethylene(EE), O, ethylene epoxide(EO) and acetyl aldehyde(AA). As PGN is chemically inert, O_2, EE, EO and AA are only physisorbed. In accordance with the upshift of Au-d states, the calculated E_{ad} for EE is -1.32 eV, which is similar to the E_{ad} of propene and is stronger than that over compact Au surfaces.[11, 18] In this configuration, the EE lies on top of the Au atom with the C=C bond in plane with one of the Au-C bonds and this plane is vertical to the EE molecule plane. The nearest Au-C(EE) distance is 2.20 Å and the H-C-H angle is also distorted from $\sim 120.0^o$ in the planar structure to 115.2^o, suggesting typical chemical bonds are formed between EE and Au and the hybridization of C(EE) atoms is changing from sp^2 to sp^3. The E_{ad} of O_2 is -1.42 eV, corresponding to O_2 lying parallel to the GN surface immediately on top of the Au atom

and the Au-O distances are both 2.17 Å. Both EE and O_2 interact strongly with AuSV, indicating that both of them can be readily adsorbed at moderate temperatures. As for O atom, it prefers to stand 1.85 Å on top of the Au atom with the Au-O direction vertical to the GN support and the corresponding E_{ad} is -4.72 eV. The enhancement of O E_{ad} can be understood as the result of lacking repulsive interaction among negative charge absorbed O atoms as compared with the case of O_2. Similar phenomena have been observed in coverage dependent O adsorption on surfaces of TMs and alloys.[67-68] The E_{ad}s of EO and AA are both enhanced moderately to -0.63 and -0.74 eV over AuSV, respectively and are in good accordance with those reported by Pulido et al.[11] In the plausible configurations, EO and AA lie in the reverse direction of one of the Au-C bonds and coordinate with Au atom with their states associated with O and the nearest Au-O distances are 2.29 and 2.19 Å, respectively.

Table 1. The E_{ad}s and the most plausible structures for reaction species adsorption on AuSV.

Species	E_{ad}^{a} (eV)	Bonding Details	
		Bond	Length (Å)
EE	-1.32	C1-C2	1.42
		Au-C1	2.20
		Au-C2	2.22
O_2^{b}	-1.42	O1-O2	1.35
		Au-O1	2.17
		Au-O2	2.17
O^{b}	-4.72	Au-O	1.85
EO	-0.63	Au-O	2.29
AA	-0.74	Au-O	2.19

[a.] The E_{ad} is calculated as the energy difference between the species adsorbed on AuSV and the gaseous species plus the bare AuSV according to equation 2.
[b] Due to the unpaired electron on Au, the ground state of AuSV is doublet. The adsorption of O_2 and O in quartet was also considered, but was found less plausible as compared with those in doublet.
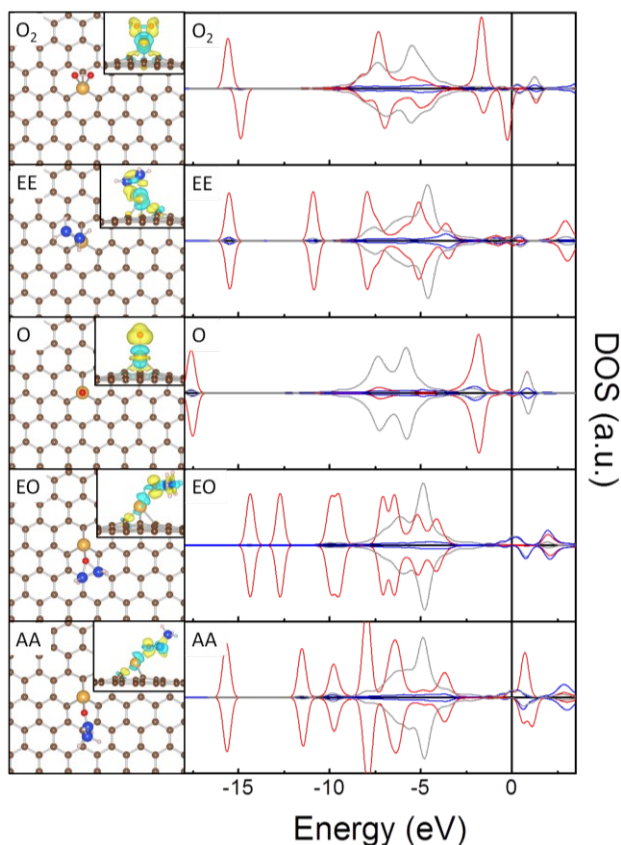
Figure 2. The most plausible adsorption structures with contour plots of differential charge density (left panel), and the corresponding DOS curves (right panel) for O_2, EE, O, EO and AA adsorption on AuSV. (C of EE: Blue; C of GN: Brown; Au: Dark yellow; O: Red; H: Pink. The contour value of the charge density is ± 0.005 a.u. The charge accumulation regions are in light yellow while the charge depletion regions are in light blue. The DOS curves of adsorbates are in red, those of Au-sp and Au-d are in blue and grey, respectively. The DOS curves are aligned by the calculated Fermi level.)

Due to the formation of Au-O and Au-C bonds, all the states of the adsorbates are downshifted and the shape and distribution of DOS peaks corresponding to frontier states of EE, O_2, EO and AA change significantly. (Figure 2c) Even some of the low lying empty states of adsorbates are split into parts and partially downshifted to below the E_F to resonance strongly with the Au-d and

Au-sp states, showing the charge transfer among them. In all the cases, the charge depletion regions reside inside the adsorbates and on AuSV while the charge accumulation regions lie between AuSV and the adsorbates (Figure 2, insets in left panel), showing the direction of the charge transfer, the partial covalent nature of the bonding and the activation of the adsorbates. The calculated amounts of charge transfer among O_2, EE, O, EO, AA and AuSV are 0.28, 0.04, 0.37, 0.15 and 0.12 |e|, respectively. These, together with the elongation of $O-O(O_2)$, C-C(EE), C-O(EO), C-O(AA) distances from 1.23, 1.34, 1.44 and 1.22 Å, respectively in free molecules to 1.35, 1.42, 1.47 and 1.25 Å, respectively after adsorption further confirm the activations of adsorbates. The weak binding, small charge transfer and slight elongation of C-O bonds in EO and AA also suggest that the desorption of EO and AA might be facile, especially when coadsorbed with O_2 or EE.

It has been reported that preactivation of O_2 to O atom is required for EE epoxidation over Ag surfaces or NPs for formation of the OMC intermediate.[67, 69] Due to the limited coordination sites, the calculated E_{ad} for 2 O atomic adsorption is 1.48 eV less stable as compared with the adsorption of O_2, implying that the direct activation of O_2 to O atom is hard to take place over AuSV.[11] As the O_2 is partially activated upon adsorption, we firstly considered the direct reaction of adsorbed O_2 with gaseous EE. Due to the charge transfer between O_2 and AuSV, the $O_2-2\pi$ states of antibonding character get occupied, become the frontier states and interact with the π antibonding states of EE for formation of a glycol like (-O-CH_2-CH_2-O-) intermediate. Though this is a 3.19 eV exothermic process, the required charge transfer from adsorbed O_2 for reaction with EE makes the barrier at least 1.75 eV, while that for scission one of the O-C bonds for formation of EO and 1 adsorbed O atom is calculated as 3.07 eV. In this sense, EE would react with adsorbed O_2 through other mechanisms.

In fact, the coadsorption of EE and O_2 is plausible over AuSV and satisfies the requirements for initiation of EE epoxidation. Previously, a similar mechanism has been proposed for the high performance of Au and Pt atoms embedded in graphene and h-BN and on Au clusters deposited over MgO and TiO_2 in CO oxidation.[48, 51, 70-71] The most plausible adsorption structure of EE and O_2, together with the atomic structures at various states along the minimum-energy path (MEP) are shown in Figure 3, with the corresponding structural parameters listed in Table 2.
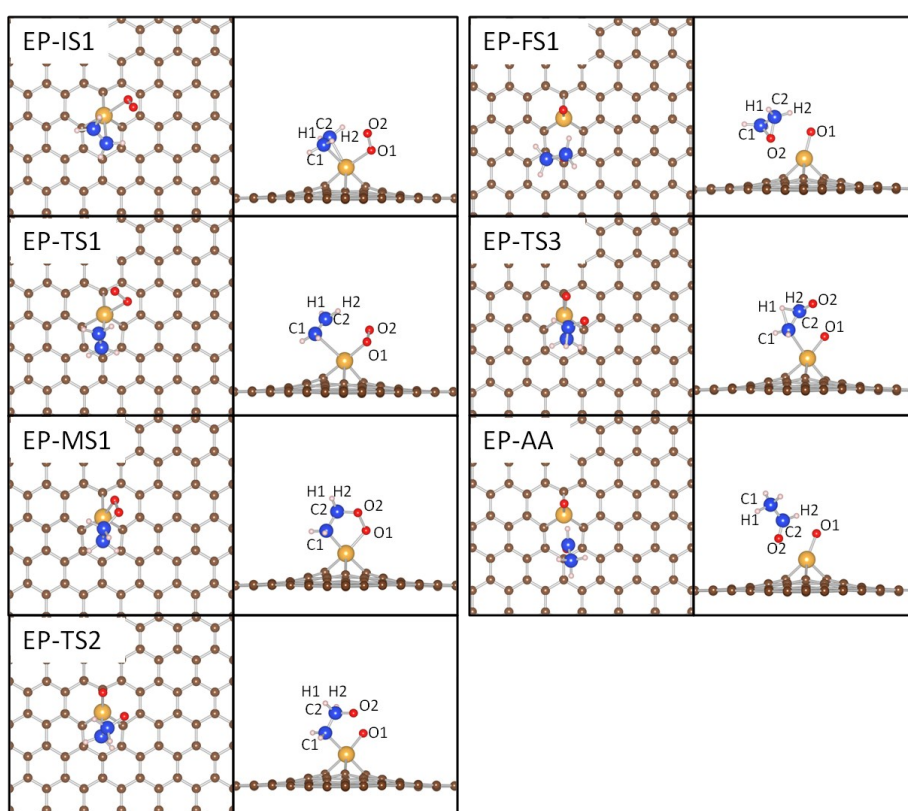

Figure 3. Top views and side views of local configurations of the adsorbates on the AuSV at various states along the MEP for EE epoxidation, including the initial state (EP-IS1), transition states (EP-TS1, EP-TS2 and EP-TS3), intermediate state (EP-MS1) and the final states (EP-FS1 and EP-AA). (C of GN: Brown; C of EE: Blue; H: Pink; O: Red; Au: Yellow.)

Table 2. Structural Parameters of Various States along the MEP for EE Epoxidation over AuSV.
a

States	$d_{O1\text{-}O2}$ (Å)	$d_{C1\text{-}C2}$ (Å)	$d_{Au\text{-}O1}$ (Å)	$d_{Au\text{-}O2}$ (Å)	$d_{Au\text{-}C1}$ (Å)	$d_{Au\text{-}C2}$ (Å)	$d_{C2\text{-}O2}$ (Å)	$\angle_{H1\text{-}C2\text{-}H2}$ (°)	$\angle_{H2\text{-}C2\text{-}O2}$ (°)
EP-IS1	1.30	1.38	2.23	3.06	2.39	2.32	2.99	117.85	45.57
EP-TS1	1.32	1.35	2.14	2.63	2.81	3.04	3.08	116.21	56.33
EP-MS1	1.45	1.52	2.05	2.94	2.15	2.89	1.43	108.82	103.10
EP-TS2	2.53	1.53	1.95	3.21	2.18	3.06	1.35	106.11	108.95
EP-FS1	3.13	1.47	1.86	2.90	3.66	3.65	1.45	117.86	113.79
EP-TS3	3.00	1.48	1.94	3.93	2.48	3.27	1.27	104.86	119.70
EP-AA	3.02	1.49	1.88	2.66	4.77	3.29	1.23	147.36	117.79

a The distance between specific atoms. Please see Figure 3 and the context for the nomination of atoms.

Though both EE and O_2 gain electrons from AuSV in the coadsorbed configuration (EP-IS1), C2 atom of EE and O2 atom of O_2 are of different spins and the major spin is localized on O_2. This drives the O2 of O_2 to move toward C2 atom of EE to reach the transition state (EP-TS1) that connects EP-IS1 to EP-MS1 on the MEP. During this endothermic process, both the structures of EE and O_2 are distorted for the C2-O2 interaction. The O1-O2 distance in O_2 is stretched from 1.30 Å in EP-IS1 to 1.32 Å in EP-TS1, while the C1-C2 distance is changed from 1.38 Å after adsorption to 1.35 Å. The energy barrier for the formation of EP-MS1 is 0.30 eV and a peroxide-like OMC complex (-O1-O2-CH$_2$-CH$_2$-) is thus formed. Because the C2-O2 interaction is mature in EP-MS1, the O1-O2 distance is further elongated to 1.45 Å. The O-O distance of this length scale has been only be observed in peroxides, showing the instability of EP-MS1 and the easiness for scission of the O-O bond. The formation of EP-MS1 is exothermic by 1.18 eV as compared with EP-TS1 and the localized spin is balanced by the formation of C2-O2 bond. As a consequence of the instable peroxide structure, EP-MS1 dissociates by breaking the O1-O2 bond and forms a weakly adsorbed EO and an O atom adsorbed on AuSV (EP-FS1). Due to the instability of both C-O bonds in EO and adsorbed O atom and the repulsive

interaction between negatively charged O2 and C1 of EE, the barrier for the formation of weakly

adsorbed EO (EP-FS1) from EP-MS1 is 0.84 eV. The tendency to strengthen the C2-O2

interaction and weaken the O1-O2 and Au-C2 interaction is already apparent at the transition

state (EP-TS2), where the O1-O2 distance is already as long as 2.53 Å, the Au-C2 distance has

reached 3.06 Å, while the C2-O2 distance is shortened from 1.43 Å to 1.35 Å. This suggests that

the dissociation of EP-MS1 is a relatively facile process and is ready to take place at moderate

condition. As the E_{ad} of EO is only -0.30 eV in existence of coadsorbed O atom, the desorption

of EO in EP-FS1 can be considered facile.

The direct attaching of O2 to AuSV for formation of coadsorbed OMC ($-O-CH_2-CH_2-$) and O

atom was found endothermic by 1.04 eV with respect to EP-MS1, so the reactions on this path

were then ruled out. We also considered the possibility for AA formation by hydride transfer

from EP-MS1. It should be noticed that the H1-Au and H2-Au distances are 3.17 and 3.91 Å in

EP-MS1. As the C2-Au distance is already 2.89 Å and the 5-member ring structure of EP-MS1 is

highly rigid, it is hard to consider there are direct interactions between AuSV and C2(EE) that

will assist the hydride transfer of H1 from C2 to C1 for the formation of AA. Resulting from this,

the path to EP-TS3 would be endothermic by 1.42 eV, though the formation of final product (EP-

AA) is 2.77 eV exothermic. This high reaction barrier makes the formation of EP-AA from EP-

MS1 a kinetically prohibited process and the limited coordination sites on AuSV due to the

mono-dispersion of Au atoms may play a role.

The subsequent reaction takes place between a gaseous EE molecule and the adsorbed O atom

over AuBV for the regeneration of Au atom as available reaction site (Figure 4 and Table 3).

The O atom would be highly reactive due to the charge and spin accumulation and has been

proposed as the key reaction intermediate in EE epoxidation on Ag and Au surfaces, especially

15

during the formation of OMC. A configuration of the EE molecule stands more than 3.0 Å away

from the adsorbed atomic O on AuSV was selected as the initial state (EP-IS2). Due to the

partially ionic nature of the O-Au bond, one of C(EE) get polarized and positively charged while

another C(EE) get negatively charged when EE is approaching the reaction site (EP-TS4). The

electrostatic C(EE)-O and C(EE)-Au interaction make the formation of OMC (EP-MS2)

exothermic by 1.33 eV and the barrier is 0.54 eV. This is similar to the barrier reported for OMC

formation over oxygenated surface of Au and Au NPs (0.49 and 0.23 eV, respectively).[25] The

slight difference in barrier height can be attributed to the fact that both O and EE gains charge

from AuSV. However, due to the enhanced Au-O and Au-C interactions in EP-MS2, the barriers

for formation of EP-FS2 and EP-FS3 by scission of Au-C and hydride transfer through EP-TS5

and EP-TS6 are already 1.45 and 2.17 eV, respectively. Similar barriers for breaking of OMC

has been reported on Au NPs while the significant difference in reaction barrier also suggests the

potential high selectivity to EO over AuSV.[25] These high barriers also imply that breaking of EP-

MS2 will slow down the subsequent reactions unless there are alternative reaction paths.

Table 3. Structural Parameters for Various States along the MEP
for reaction of the gaseous EE with adsorbed O atom over AuSV.[a]

States	d_{C1-C2} (Å)	d_{O1-C1} (Å)	d_{O1-C2} (Å)	d_{Au-O1} (Å)	$\angle_{H1-C1-H2}$ (°)	$\angle_{H2-C1-O1}$ (°)
EP-IS2	1.34	3.40	3.52	1.85	116.4	95.1
EP-TS4	1.36	2.41	3.19	1.93	116.6	85.3
EP-MS2	1.52	1.45	2.34	2.04	107.9	108.7
EP-TS5	1.48	1.45	2.38	2.02	108.0	105.8
EP-FS2	1.47	1.47	1.47	2.29	116.7	114.4
EP-TS6	1.45	1.31	2.42	2.21	100.7	117.2
EP-FS3	1.48	1.25	2.39	2.19	146.8	119.6
EP-TS7	1.48	1.44	2.42	2.05	106.6	104.9

[a] The distance between specific atoms. Please see Figure 4 and the
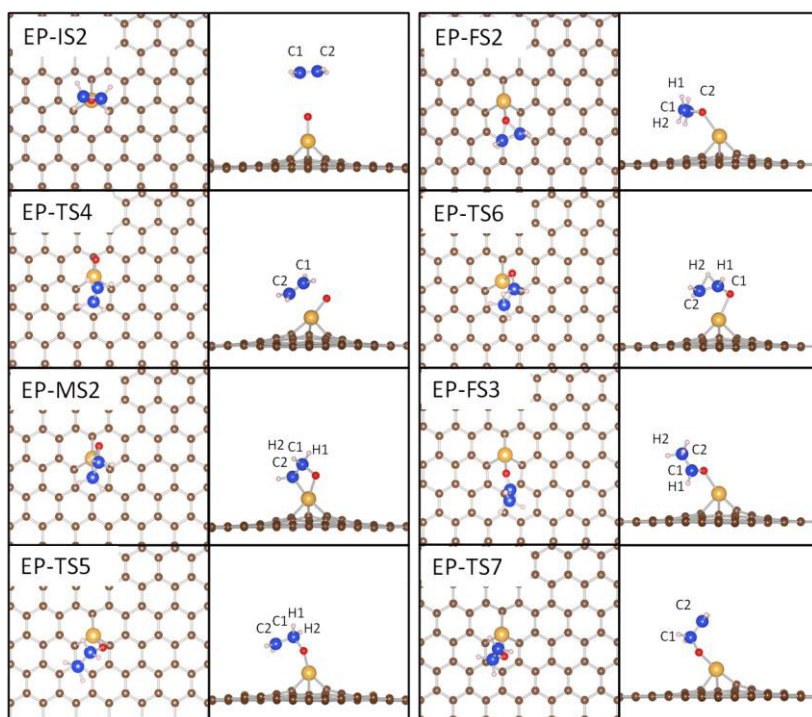context for the nomination of atoms.

Figure 4. Top views and side views of local configurations of the adsorbates on the AuSV at various states along the MEP for reaction of gaseous EE with remnant O atom, including the initial state (EP-IS2), transition states (EP-TS4, EP-TS5, EP-TS6 and EP-TS7), intermediate state (EP-MS2) and the final states (EP-FS2 and EP-FS3). (C of GN: Brown; C of EE: Blue; H: Pink; O: Red; Au: Yellow.)

It has been reported that the oxidation of EE can also take place by reaction of adsorbed O atom and gaseous EE for direct formation of EO and this is also the mechanism for EE oxidation over TM complexes and oxygenated $Ag_2O(001)$ surface.[72-74] The configuration that EO adsorbed on AuSV (EP-FS2) was set as the final state. Due to the charge accumulation on the remnant O atom, when the gaseous EE approaches to AuSV, the C atom of EE gets partially positively charged and interacts electrostatically with the remnant O atom to reach EP-TS7. Within EP-TS7, the C1-O1 distance is decreased from 3.40 Å in EP-IS2 to 1.44 Å and the Au-C1 distance is also decreased from 5.20 to 3.08 Å, showing that EE is pushed to the AuSV in this endothermic

process due to the interaction between C1(EE) and O1 atom. Because of the high reactivity of the adsorbed O atom and the strong exothermicity for formation of C-O bonds, the reaction barrier for formation of EP-FS2 is as low as 0.18 eV and the reaction is exothermic by 0.57 eV with respect to EP-TS7. We also investigated the AA formation (EP-FS3) from the unactivated EE as a process competing with that of EO, but the calculated barrier is as high as 3.05 eV. In this sense, the formation of AA from EP-IS2 would also be a kinetically forbidden process and EO will be the dominant product. This is similar to EO formation over oxygenated Ag_2O (001) where the surface oxide structure limits the binding of ethylene with Ag cations for AA formation.[74] Following the EO formation, O_2 and EE adsorption will take place for formation of coadsorption structures or even compete with the adsorption of EO. We investigated the coadsorption of EO with O_2 and EE and found that E_{ad} of EO is decreased to -0.18 and -0.30 eV, respectively, which implies the desorption of EO and the proceeding of the reaction facile.
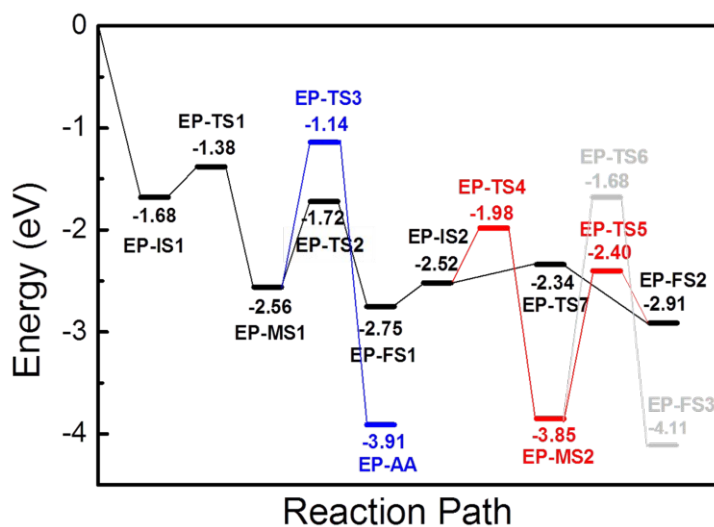

Figure 5. Schematic energy profile corresponding to local configurations shown in Figures 3, and Figure 4 along the MEP for EE epoxidation over AuSV. All energies are given with respect to the reference energy, i.e., the sum of energies of the clean AuSV and gaseous EE and O_2 molecules.

In summary, the EE epoxidation over AuSV may be characterized as the following: The EE catalytic epoxidation cycle is initiated with reaction of the coadsorbed EE and O_2 (EP-IS1) to form a peroxide like complex (EP-MS1), by the dissociation of which the an EO molecule and an adsorbed O atom are formed (EP-FS1), and then the AuSV is regenerated to be available by the reaction of a gaseous EE with the adsorbed O atom (EP-IS2) to form another EO (EP-FS2).(Figure 5) We investigated the evolution of DOS of EE and O_2 during the reaction (Figure S1) and realized that the potential high catalytic performance of AuSV can be attributed to the compatibility of the states of AuSV and adsorbed intermediates, particularly among the upshifted Au-d states originated from the interfacial Au-C interactions and the molecular states of EE and O_2, that facilitates the required charge transfer for the reaction to proceed. The limited binding sites resulting from the mono-dispersion of the Au atoms differentiates the reaction barriers for formation of EO and AA and accounts for the potentially high selectivity to EO.[74]

4. CONCLUSION

We performed a first-principles-based investigation on the potential catalytic role of Au atoms dispersed on graphene in ethylene epoxidation. We showed the Au atom binds strongly onto the vacancy on graphene and the outward diffusing of the Au atom is endothermic by 2.10 eV, which make the diffusion and aggregation of these monodispersed Au atoms a kinetically prohibited process in conventional conditions. This strong interfacial interaction also tunes the energy level of Au-d states for the activation of O_2 and EE and promotes the formation and dissociation of the peroxametallacycle intermediate. The ethylene epoxidation over AuSV involves the formation of a peroxametallacycle intermediate by the coadsorbed EE and O_2, the dissociation of the peroxametallacycle intermediate for formation of an EO molecule and an adsorbed O atom, the direct reaction of another gaseous EE with the remnant O atom for the

formation of EO and the coadsorption of EE or O_2 that facilitates the EO desorption and acts as the initiation of another reaction cycle. The calculated barriers for the formation and dissociation of oxametallacycle intermediate and regeneration of Au site are 0.30, 0.84 and 0.18 eV, respectively and are significantly lower than those for aldehyde formation, indicating the potential high catalytic performance of these mono-dispersed Au atoms for ethylene epoxidation. These findings also highlight the possibility to regulate the selectivity of structure sensitive reactions by limiting the coordination and interaction of the TM centers with the reaction intermediates and would be helpful for future design and implementation of high performance single-atom catalysts.

AUTHOR INFORMATION

Corresponding Authors

*Dr. Xin Liu and Prof. Yu Han

Tel: +86-411-84986343(X. L.); +966-2-8082407

Email: xliu@dlut.edu.cn (X. L.); yu.han@kaust.edu.sa (Y. H.)

Author Contributions

X. L. designed the research after discussion with Y.H. and C. M. and wrote the manuscript. Y. Y. conceived the calculations and analyzed the results with the assistance of M. C. and T. D. Y. Y. is responsible for the calculation results. Y. H. and C. M. proofed the manuscript and polished the language. All authors have given approval to the final version of the manuscript.

REFERENCES

1.   Dever, J. P.; George, K. F.; Hoffman, W. C.; Soo, H., Ethylene Oxide. In *Kirk-Othmer Encyclopedia of Chemical Technology*, John Wiley & Sons, Inc.: 2000.
2.   Linic, S.; Barteau, M. A., Control of Ethylene Epoxidation Selectivity by Surface Oxametallacycles. *J. Am. Chem. Soc.* **2003**, *125*, 4034-4035.
3.   Linic, S.; Barteau, M. A., Formation of a Stable Surface Oxametallacycle That Produces Ethylene Oxide. *J. Am. Chem. Soc.* **2002**, *124*, 310-317.
4.   Ethylene Oxide (Eo) - a Global Strategic Business Report. Global Industry Analysis, Inc.: 2012; p 360.
5.   Linic, S.; Barteau, M. A., Construction of a Reaction Coordinate and a Microkinetic Model for Ethylene Epoxidation on Silver from Dft Calculations and Surface Science Experiments. *J. Catal.* **2003**, *214*, 200-212.
6.   Linic, S.; Jankowiak, J.; Barteau, M. A., Selectivity Driven Design of Bimetallic Ethylene Epoxidation Catalysts from First Principles. *J. Catal.* **2004**, *224*, 489-493.
7.   Liu, X. Y.; Klust, A.; Madix, R. J.; Friend, C. M., Structure Sensitivity in the Partial Oxidation of Styrene, Styrene Oxide, and Phenylacetaldehyde on Silver Single Crystals. *J. Phys. Chem. C* **2007**, *111*, 3675-3679.
8.   Campbell, C. T., The Selective Epoxidation of Ethylene Catalyzed by Ag(111) - a Comparison with Ag(110). *J. Catal.* **1985**, *94*, 436-444.
9.   Christopher, P.; Linic, S., Engineering Selectivity in Heterogeneous Catalysis: Ag Nanowires as Selective Ethylene Epoxidation Catalysts. *J. Am. Chem. Soc.* **2008**, *130*, 11264-+.
10.   Christopher, P.; Linic, S., Shape- and Size-Specific Chemistry of Ag Nanostructures in Catalytic Ethylene Epoxidation. *ChemCatChem* **2010**, *2*, 78-83.
11.   Pulido, A.; Boronat, M.; Corma, A., Propene Epoxidation with H2/H2o/O2 Mixtures over Gold Atoms Supported on Defective Graphene: A Theoretical Study. *The Journal of Physical Chemistry C* **2012**.
12.   Linic, S.; Christopher, P., Overcoming Limitation in the Design of Selective Solid Catalysts by Manipulating Shape and Size of Catalytic Particles: Epoxidation Reactions on Silver. *ChemCatChem* **2010**, *2*, 1061-1063.
13.   Garcia-Mota, M.; Rieger, M.; Reuter, K., Ab Initio Prediction of the Equilibrium Shape of Supported Ag Nanoparticles on Alpha-Al2o3(0001). *J. Catal.* **2015**, *321*, 1-6.

14.   Diao, W. J.; DiGiulio, C. D.; Schaal, M. T.; Ma, S. G.; Monnier, J. R., An Investigation on the Role of Re as a Promoter in Ag-Cs-Re/Alpha-Al2o3 High-Selectivity, Ethylene Epoxidation Catalysts. *J. Catal.* **2015**, *322*, 14-23.

15.   Piccinin, S.; Nguyen, N. L.; Stampfl, C.; Scheffler, M., First-Principles Study of the Mechanism of Ethylene Epoxidation over Ag-Cu Particles. *J. Mater. Chem.* **2010**, *20*, 10521-10527.

16.   Piccinin, S., et al., Alloy Catalyst in a Reactive Environment: The Example of Ag-Cu Particles for Ethylene Epoxidation. *Phys. Rev. Lett.* **2010**, *104*.

17.   Lei, Y., et al., Increased Silver Activity for Direct Propylene Epoxidation Via Subnanometer Size Effects. *Science* **2010**, *328*, 224-228.

18.   Torres, D.; Illas, F., On the Performance of Au(111) for Ethylene Epoxidation: A Density Functional Study. *J. Phys. Chem. B* **2006**, *110*, 13310-13313.

19.   Haruta, M., Catalysis - Gold Rush. *Nature* **2005**, *437*, 1098-1099.

20.   Turner, M.; Golovko, V. B.; Vaughan, O. P. H.; Abdulkin, P.; Berenguer-Murcia, A.; Tikhov, M. S.; Johnson, B. F. G.; Lambert, R. M., Selective Oxidation with Dioxygen by Gold Nanoparticle Catalysts Derived from 55-Atom Clusters. *Nature* **2008**, *454*, 981-U31.

21.   Haruta, M., Size- and Support-Dependency in the Catalysis of Gold. *Catal. Today* **1997**, *36*, 153-166.

22.   Hayashi, T.; Tanaka, K.; Haruta, M., Selective Vapor-Phase Epoxidation of Propylene over Au/Tio2 Catalysts in the Presence of Oxygen and Hydrogen. *J. Catal.* **1998**, *178*, 566-575.

23.   Nakatsuji, H.; Hu, Z. M.; Nakai, H.; Ikeda, K., Activation of O-2 on Cu, Ag, and Au Surfaces for the Epoxidation of Ethylene: Dipped Adcluster Model Study. *Surf. Sci.* **1997**, *387*, 328-341.

24.   Chang, C. R.; Wang, Y. G.; Li, J., Theoretical Investigations of the Catalytic Role of Water in Propene Epoxidation on Gold Nanoclusters: A Hydroperoxyl-Mediated Pathway. *Nano Res.* **2011**, *4*, 131-142.

25.   Chen, H. T.; Chang, J. G.; Ju, S. P.; Chen, H. L., Ethylene Epoxidation on a Au Nanoparticle Versus a Au(111) Surface: A Dft Study. *J. Phys. Chem. Lett.* **2010**, *1*, 739-742.

26.   Lyalin, A.; Taketsugu, T., Reactant-Promoted Oxygen Dissociation on Gold Clusters. *J. Phys. Chem. Lett.* **2010**, *1*, 1752-1757.

27.   Pulido, A.; Boronat, M.; Corma, A., Theoretical Investigation of Gold Clusters Supported on Graphene Sheets. *New J. Chem.* **2011**, *35*, 2153-2161.

28.   Yang, X. F.; Wang, A. Q.; Qiao, B. T.; Li, J.; Liu, J. Y.; Zhang, T., Single-Atom Catalysts: A New Frontier in Heterogeneous Catalysis. *Accounts Chem. Res.* **2013**, *46*, 1740-1748.

29.   Hammer, B.; Norskov, J. K., Theoretical Surface Science and Catalysis - Calculations and Concepts. In *Advances in Catalysis*, Academic Press Inc: San Diego, 2000; Vol. 45, pp 71-129.

30.   Remediakis, I. N.; Lopez, N.; Norskov, J. K., Co Oxidation on Rutile-Supported Au Nanoparticles. *Angew. Chem.-Int. Edit.* **2005**, *44*, 1824-1826.

31.   Li, L.; Larsen, A. H.; Romero, N. A.; Morozov, V. A.; Glinsvad, C.; Abild-Pedersen, F.; Greeley, J.; Jacobsen, K. W.; Norskov, J. K., Investigation of Catalytic Finite-Size-Effects of Platinum Metal Clusters. *J. Phys. Chem. Lett.* **2013**, *4*, 222-226.

32.   Liu, X.; Sui, Y.; Meng, C.; Han, Y., Tuning the Reactivity of Ru Nanoparticles by Defect Engineering of the Reduced Graphene Oxide Support. *RSC Adv.* **2014**, *4*, 22230-22240.

33.   Liu, X.; Meng, C.; Han, Y., Substrate-Mediated Enhanced Activity of Ru Nanoparticles in Catalytic Hydrogenation of Benzene. *Nanoscale* **2012**, *4*, 2288-2295.

34.   Chen, M. S.; Goodman, D. W., Catalytically Active Gold on Ordered Titania Supports. *Chem. Soc. Rev.* **2008**, *37*, 1860-1870.

35.   Yao, Y. X.; Liu, X.; Fu, Q.; Li, W. X.; Tan, D. L.; Bao, X. H., Unique Reactivity of Confined Metal Atoms on a Silicon Substrate. *ChemPhysChem* **2008**, *9*, 975-979.

36.   Uzun, A.; Ortalan, V.; Hao, Y. L.; Browning, N. D.; Gates, B. C., Nanoclusters of Gold on a High-Area Support: Almost Uniform Nanoclusters Imaged by Scanning Transmission Electron Microscopy. *ACS Nano* **2009**, *3*, 3691-3695.

37.   Qiao, B.; Liu, J.; Wang, Y.-G.; Lin, Q.; Liu, X.; Wang, A.; Li, J.; Zhang, T.; Liu, J., Highly Efficient Catalysis of Preferential Oxidation of Co in H2-Rich Stream by Gold Single-Atom Catalysts. *ACS Catalysis* **2015**, *5*, DOI: 10.1021/acscatal.5b01114.

38.   Qiao, B. T.; Wang, A. Q.; Yang, X. F.; Allard, L. F.; Jiang, Z.; Cui, Y. T.; Liu, J. Y.; Li, J.; Zhang, T., Single-Atom Catalysis of Co Oxidation Using Pt(1)/Feo(X). *Nat. Chem.* **2011**, *3*, 634-641.

39.   Zhang, X.; Shi, H.; Xu, B. Q., Catalysis by Gold: Isolated Surface Au3+ Ions Are Active Sites for Selective Hydrogenation of 1,3-Butadiene over Au/Zro2 Catalysts. *Angew. Chem.-Int. Edit.* **2005**, *44*, 7132-7135.

40.   Ding, W. C.; Gu, X. K.; Su, H. Y.; Li, W. X., Single Pd Atom Embedded in Ceo2(111) for No Reduction with Co: A First-Principles Study. *J. Phys. Chem. C* **2014**, *118*, 12216-12223.

41.   Lin, J.; Qiao, B. T.; Liu, J. Y.; Huang, Y. Q.; Wang, A. Q.; Li, L.; Zhang, W. S.; Allard, L. F.; Wang, X. D.; Zhang, T., Design of a Highly Active Ir/Fe(Oh)X Catalyst: Versatile Application of Pt-Group Metals for the Preferential Oxidation of Carbon Monoxide. *Angew. Chem.-Int. Edit.* **2012**, *51*, 2920-2924.

42.   Hu, P. P.; Huang, Z. W.; Amghouz, Z.; Makkee, M.; Xu, F.; Kapteijn, F.; Dikhtiarenko, A.; Chen, Y. X.; Gu, X.; Tang, X. F., Electronic Metal- Support Interactions in Single- Atom Catalysts. *Angew. Chem.-Int. Edit.* **2014**, *53*, 3418-3421.

43.   Guo, X., et al., Direct, Nonoxidative Conversion of Methane to Ethylene, Aromatics, and Hydrogen. *Science* **2014**, *344*, 616-619.

44.   Krasheninnikov, A. V.; Lehtinen, P. O.; Foster, A. S.; Pyykko, P.; Nieminen, R. M., Embedding Transition-Metal Atoms in Graphene: Structure, Bonding, and Magnetism. *Phys. Rev. Lett.* **2009**, *102*, 126807.

45.   Liu, X.; Meng, C. G.; Han, Y., Substrate-Mediated Enhanced Activity of Ru Nanoparticles in Catalytic Hydrogenation of Benzene. *Nanoscale* **2012**, *4*, 2288-2295.

46.   Liu, X.; Li, L.; Meng, C. G.; Han, Y., Palladium Nanoparticles/Defective Graphene Composites as Oxygen Reduction Electrocatalysts: A First-Principles Study. *J. Phys. Chem. C* **2012**, *116*, 2710-2719.

47.   Wang, H., et al., Doping Monolayer Graphene with Single Atom Substitutions. *Nano Lett.* **2011**, *12*, 141-144.

48.   Lu, Y. H.; Zhou, M.; Zhang, C.; Feng, Y. P., Metal-Embedded Graphene: A Possible Catalyst with High Activity. *J. Phys. Chem. C* **2009**, *113*, 20156-20160.

49.   Li, Y.; Zhou, Z.; Yu, G.; Chen, W.; Chen, Z., Co Catalytic Oxidation on Iron-Embedded Graphene: Computational Quest for Low-Cost Nanocatalysts. *J. Phys. Chem. C* **2010**, *114*, 6250-6254.

50.   Song, E. H.; Wen, Z.; Jiang, Q., Co Catalytic Oxidation on Copper-Embedded Graphene. *J. Phys. Chem. C* **2011**, *115*, 3678-3683.

51.   Liu, X.; Sui, Y.; Duan, T.; Meng, C.; Han, Y., Co Oxidation Catalyzed by Pt-Embedded Graphene: A First-Principles Investigation. *Phys. Chem. Chem. Phys.* **2014**, *16*, 23584-23593.

52.   Delley, B., An All-Electron Numerical-Method for Solving the Local Density Functional for Polyatomic-Molecules. *J. Chem. Phys.* **1990**, *92*, 508-517.

53.   Delley, B., From Molecules to Solids with the Dmol(3) Approach. *J. Chem. Phys.* **2000**, *113*, 7756-7764.

54.   Perdew, J. P.; Burke, K.; Ernzerhof, M., Generalized Gradient Approximation Made Simple. *Phys. Rev. Lett.* **1996**, *77*, 3865-3868.

55.   Delley, B., Hardness Conserving Semilocal Pseudopotentials. *Phys. Rev. B* **2002**, *66*, 155125.

56.   Liu, X.; Meng, C. G.; Liu, C. H., Molecular Dynamics Study on Superheating of Pd at High Heating Rates. *Phase Transit.* **2006**, *79*, 249-259.

57.   Liu, X.; Meng, C. G.; Liu, C. H., Melting and Superheating of Ag at High Heating Rate. *Acta Phys.-Chim. Sin.* **2004**, *20*, 280-284.

58.   Govind, N.; Petersen, M.; Fitzgerald, G.; King-Smith, D.; Andzelm, J., A Generalized Synchronous Transit Method for Transition State Location. *Comput. Mater. Sci.* **2003**, *28*, 250-258.

59.   Monkhorst, H. J.; Pack, J. D., Special Points for Brillouin-Zone Integrations. *Phys. Rev. B* **1976**, *13*, 5188-5192.

60.   Hirshfeld, F. L., Bonded-Atom Fragments for Describing Molecular Charge-Densities. *Theor. Chim. Acta* **1977**, *44*, 129-138.

61.   Castro Neto, A. H.; Guinea, F.; Peres, N. M. R.; Novoselov, K. S.; Geim, A. K., The Electronic Properties of Graphene. *Rev Mod Phys* **2009**, *81*, 109-162.

62.   Uzun, A.; Ortalan, V.; Browning, N. D.; Gates, B. C., A Site-Isolated Mononuclear Iridium Complex Catalyst Supported on Mgo: Characterization by Spectroscopy and Aberration-Corrected Scanning Transmission Electron Microscopy. *J. Catal.* **2010**, *269*, 318-328.

63.   Gomez-Navarro, C.; Meyer, J. C.; Sundaram, R. S.; Chuvilin, A.; Kurasch, S.; Burghard, M.; Kern, K.; Kaiser, U., Atomic Structure of Reduced Graphene Oxide. *Nano Lett.* **2010**, *10*, 1144-1148.

64.   Liu, X.; Meng, C. G.; Han, Y., Defective Graphene Supported Mpd12 (M = Fe, Co, Ni, Cu, Zn, Pd) Nanoparticles as Potential Oxygen Reduction Electrocatalysts: A First-Principles Study. *J. Phys. Chem. C* **2013**, *117*, 1350-1357.

65.   Chan, B.; Yim, W. L., Accurate Computation of Cohesive Energies for Small to Medium-Sized Gold Clusters. *J. Chem. Theory Comput.* **2013**, *9*, 1964-1970.

66.   Qiao, B. T.; Liang, J. X.; Wang, A. Q.; Xu, C. Q.; Li, J.; Zhang, T.; Liu, J. Y., Ultrastable Single-Atom Gold Catalysts with Strong Covalent Metal-Support Interaction (Cmsi). *Nano Res.* **2015**, *8*, 2913-2924.

67.   Li, W. X.; Stampfl, C.; Scheffler, M., Oxygen Adsorption on Ag(111): A Density-Functional Theory Investigation. *Phys. Rev. B* **2002**, *65*, 075407.

68.   Liu, X.; Guo, H.; Meng, C., Oxygen Adsorption and Diffusion on Niti Alloy (100) Surface: A Theoretical Study. *J. Phys. Chem. C* **2012**, *116*, 21771-21779.

69.   Li, W. X.; Stampfl, C.; Scheffler, M., Why Is a Noble Metal Catalytically Active? The Role of the O-Ag Interaction in the Function of Silver as an Oxidation Catalyst. *Phys. Rev. Lett.* **2003**, *90*, 256102.
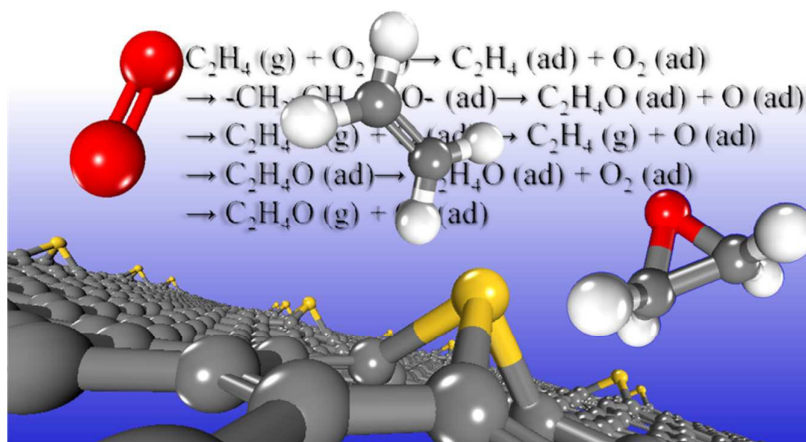

70.   Liu, Z.-P.; Hu, P.; Alavi, A., Catalytic Role of Gold in Gold-Based Catalysts: A Density Functional Theory Study on the Co Oxidation on Gold. *J. Am. Chem. Soc.* **2002**, *124*, 14770-14779.

71.   Liu, C.; Tan, Y.; Lin, S.; Li, H.; Wu, X.; Li, L.; Pei, Y.; Zeng, X. C., Co Self-Promoting Oxidation on Nanosized Gold Clusters: Triangular Au3 Active Site and Co Induced O–O Scission. *J. Am. Chem. Soc.* **2013**, *135*, 2583-2595.

72.   McGarrigle, E. M.; Gilheany, D. G., Chromium- and Manganese-Salen Promoted Epoxidation of Alkenes. *Chem. Rev.* **2005**, *105*, 1563-1602.

73.   Yan, W. J.; Ramanathan, A.; Ghanta, M.; Subramaniam, B., Towards Highly Selective Ethylene Epoxidation Catalysts Using Hydrogen Peroxide and Tungsten-or Niobium-Incorporated Mesoporous Silicate (Kit-6). *Catal. Sci. Technol.* **2014**, *4*, 4433-4439.

74.   Ozbek, M. O.; Onal, I.; van Santen, R. A., Ethylene Epoxidation Catalyzed by Silver Oxide. *ChemCatChem* **2011**, *3*, 150-153.

Defect Stabilized Gold Atoms on Graphene as Potential Catalysts for Ethylene Epoxidation: A First-principles Investigation

Xin Liu†, Yang Yang†, Minmin Chu†, Ting Duan†, Changgong Meng† and Yu Han‡,**

† School of Chemistry, State Key Laboratory of Fine Chemicals, Dalian University of Technology, Dalian, 116024, P. R. China.

‡ Physical Sciences and Engineering Division, Advanced Membranes and Porous Materials Center, King Abdullah University of Science and Technology, Thuwal, 23955-6900, Saudi Arabia

$$C_2H_4 (g) + O_2 \rightarrow C_2H_4 (ad) + O_2 (ad)$$
$$\rightarrow -CH_2CH_2O- (ad) \rightarrow C_2H_4O (ad) + O (ad)$$
$$\rightarrow C_2H_4 (g) + (ad) \rightarrow C_2H_4 (g) + O (ad)$$
$$\rightarrow C_2H_4O (ad) \rightarrow C_2H_4O (ad) + O_2 (ad)$$
$$\rightarrow C_2H_4O (g) + (ad)$$

The defects on graphene make Au atoms active while monodispersed and superior for ethylene epoxidation.

*Corresponding Authors:

Dr. Xin Liu and Prof. Yu Han

Tel: +86-411-84986343(X. L.); +966-2-8082407 (Y. H.)

Email: xliu@dlut.edu.cn (X. L.); yu.han@kaust.edu.sa (Y. H.)